BULETINUL INSTITUTULUI POLITEHNIC DIN IAŞI
Publicat de
Universitatea Tehnică „Gheorghe Asachi” din Iaşi
Tomul LXI (LXV), Fasc. 4, 2015
Secția
ELECTROTEHNICĂ. ENERGETICĂ. ELECTRONICĂ

MAGNETIC FIELD MODELS FOR A DC TORQUE MOTOR

BY

IOANA IONICA[1,2,*], MIRCEA MODREANU[1], ALEXANDRU MOREGA[2] and CRISTIAN BOBOC[1]

[1]National Institute for Research and Development in Electrical Engineering ICPE, Bucharest, Romania
[2]University POLITEHNICA of Bucharest, Romania

Received: November 20, 2015
Accepted for publication: December 11, 2015

Abstract. This paper aims to present and analyze magnetic field models for a DC Torque Motor, size 16, by using an electromagnetic field analysis program, which is based on the finite element method that facilitates the accurate evaluation of several configurations, reducing thus the need for experimental models.

Key words: DC torque motor; magnetic field; numerical modeling: finite element method.

1. Introduction

DC Torque Motors (DC-TM) are brushless DC motors designed to work in direct-drive constructions, for instance in applications involving rotational motion over a specific operating range (Obreja & Edu, 2011). They do not require additional mechanical transmission elements such as flexible couplings and gearboxes (Upadhyay *et al.*, 2003; Upadhyay & Rajagopal, 2006; Upadhyay & Rajagopal, 2005). The static friction torque is very small and the pending mechanical friction is absent, which recommend them for high performance, limited angle drives (Andrei & Modreanu, 2014).

This paper presents magnetic field models for DC-TMs, size 16 (Figs. 1 and 2), using the Finite Element Method (http://www.comsol.com/) aimed to obtain higher electromagnetic torque and higher uniformity degree of the torque-angle characteristic for the operating range through properly

[*]Corresponding author : *e-mail*: ioana.messico@icpe.ro

dimensioning all parts of the motor and using optimally the total volume (Upadhyay & Rajagopal, 2005).

The magnetic field sources are the current carrying stator windings and the rare earths (NdFeB <Neodymium-Iron-Boron>) rotor permanent magnets. The main input data is: the axial length of the motor, the outer diameter of the stator, the inner diameter of the rotor, the peak current, the maximum torque, the torque at $\pm\alpha$, and the number of poles (Upadhyay *et al.*, 2003). Their sizes will be calculated first using analytical formulas and then the *B-H* curves of the ferromagnetic materials.

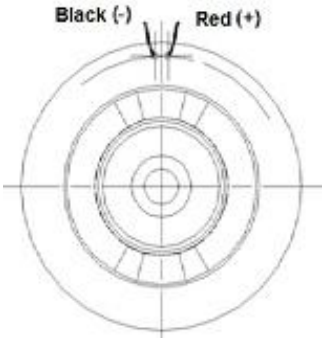

Fig. 1 – The motor structure (Andrei & Modreanu, 2014).

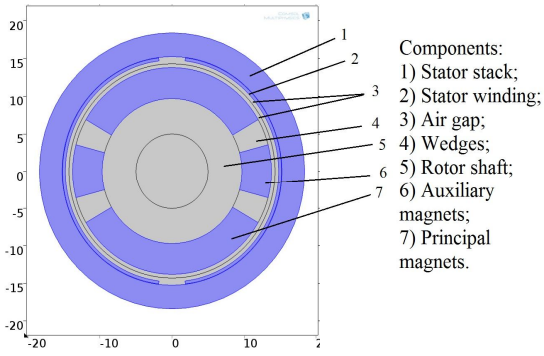

Fig. 2 – The constructive parts of the motor.

The electromagnetic torque is the main functional parameter of this motor and it is calculated here using (Raport tehnic, etapa 1; Hemeida & Sergeant, 2014; Măgureanu, 2002)

$$M = 2pR_{\text{rot}}F_{\text{pole}}, \tag{1}$$

where p is the number of pairs of poles, R_{rot} – the rotor outer radius, [m], and F_{pole} – electromagnetic force per pole, [N], defined by (Raport tehnic, etapa 1);

$$F_{\text{pole}} = B_{\delta}N\frac{\alpha_p}{\tau}I_p l_{\text{pack}}, \tag{2}$$

where: B_{δ} is the average magnetic flux density in the air gap through the magnet opening α_p, [T], N – number of conductors of a coil (per pole), τ – the polar step, I_p – the current in the coil, and l_{pack} the stator package length, [A].

We use the iterative algorithm for calculating the main parameters of the motor presented in Raport tehnic, etapa 1, which provides also the input data for a mathematical model of the magnetic field - size, material properties, magnetic field sources (Raport tehnic, etapa 2; Andrei *et al.*, 2014), that is numerically, FEM-solved (http://www.comsol.com/; Jin, 2002). We consider here only the parts that matter from the magnetic point of view, including the field sources, and use the stationary model made of

Magnetic circuit law

$$\nabla \times \mathbf{H} = \mathbf{J}, \tag{3}$$

Magnetic flux law

$$\nabla \cdot \mathbf{B} = 0 \rightarrow \mathbf{B} = \nabla \times \mathbf{A}, \tag{4}$$

Constitutive law

$$\mathbf{B} = \mu_0 \mu_r \mathbf{H} + \mathbf{B}_r. \tag{5}$$

where: **H** is the magnetic field strength, [A/m], **J** – the current density, [A/m^2], **B** – magnetic flux density, [T], **A** – the magnetic vector potential, [T·m], $\mathbf{B}_r$ – the remanent magnetic flux density (within the permanent magnets), [T], μ_0 – magnetic permeability of vacuum, [H/m], and μ_r – relative magnetic permeability.

It is customary to use the magnetic vector potential, defined through $\mathbf{B} = \nabla \times \mathbf{A}$. Then eqs. (3),…,(5) yield

$$\nabla \times \left(\mu_0^{-1} \mu_r^{-1} \left(\nabla \times \mathbf{A} - \mathbf{B}_r \right) \right) = \mathbf{J}. \tag{6}$$

The sources are to be considered within their specific domains.

The boundary condition that closes the problem is magnetic insulation, $\mathbf{n} \times \mathbf{A} = 0$, where **n** is the outer normal, allover the boundary (the outline of the stator casing).

2. Numerical Simulation Results

We study the stator and the rotor shown in Fig. 2. The materials are ferromagnetic iron, for the rotor yoke and wedges, Cobalt-Iron electrotechnic sheet, for the stator stack, and copper for the windings.

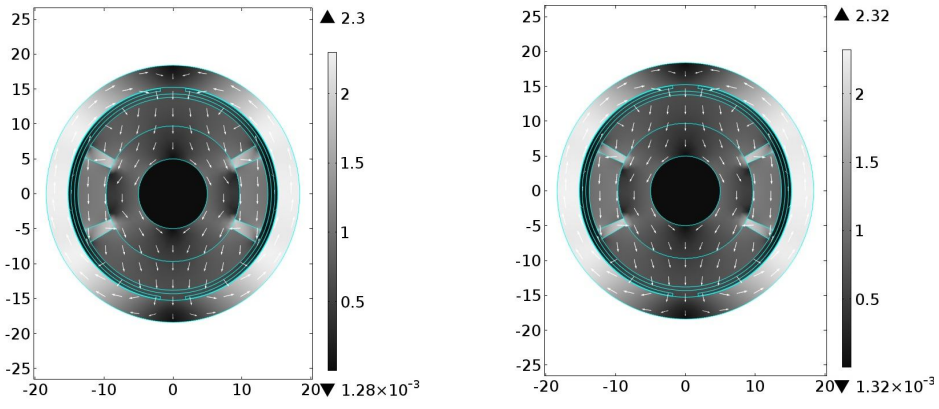

a *b*

Fig. 3 – Magnetic flux density for Iron wedges in teslas: *a* – "Design 5"; *b* – "Design 6". Dimensions are in millimetres.

We analyzed different models, evaluated the armature reaction, the saturation levels, etc., to find the design with the best performances that optimizes the motor from its design phase. Therefore starting with the initial design "1", based on which an experimental model was built, different designs of the rotor obtained by resizing the auxiliary magnets were analyzed: Iron for wedges (Fig. 3), and Aluminum wedges (nonmagnetic material) (Fig. 4).

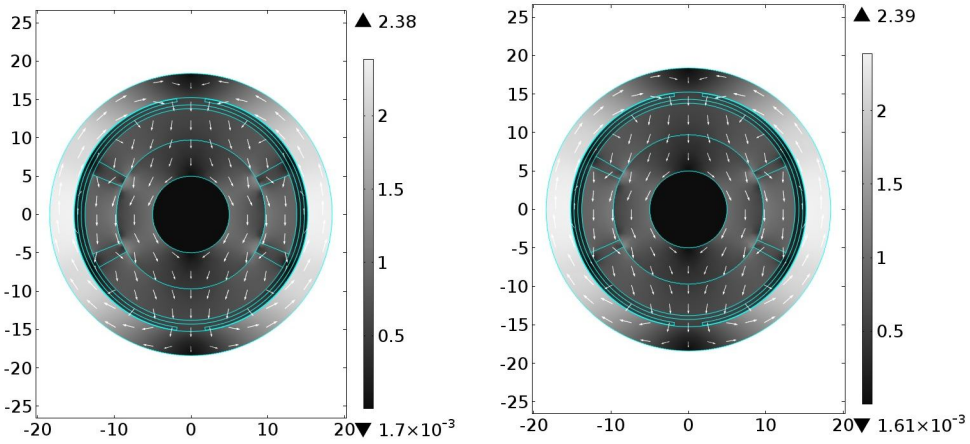

Fig. 4 – Magnetic flux density for Aluminum wedges, in teslas: *a* – "Design 5"; *b* – "Design 6". Dimensions are in millimetres.

The magnetic flux density field is confined within the Iron core while the non-magnetic regions are completely avoided (Fig. 4). The torque-angle curves for iron and aluminum wedges, designs 1–7 were computed, but it is presented only the relevant solution for each case (iron and aluminum wedges) (Fig. 5), whose numerical solution are presented in previous figure, Fig. 5.

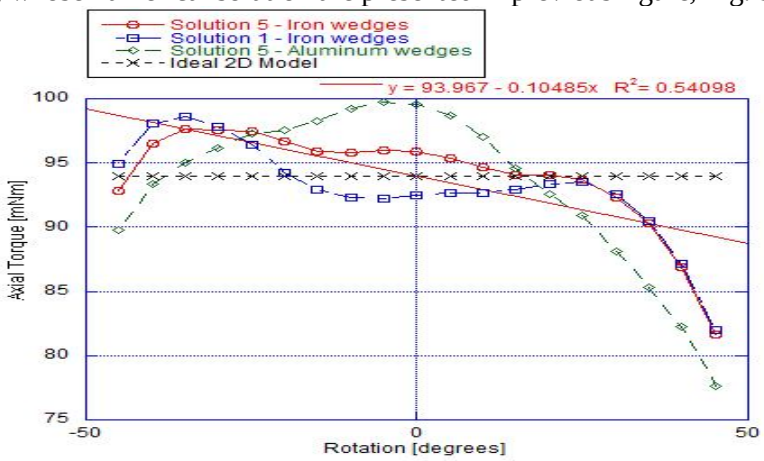

Fig. 5 – Torque-angle characteristics for Iron and Aluminum wedges.

In the Iron wedges designs, as the wedges angle decreases in a specific angular domain (working field), the torque-angle characteristic is approximately linear (Fig. 5). The torque-angle characteristics depart from linearity as the Aluminum wedges angle decreases, whereas the torque increases, as compared to Iron wedges (Fig. 5). The deviation of the torque angle characteristic on the operating range of the motor, calculate thorough

$$d = \frac{M_{\text{real}} - M_{\text{ideal}}}{M_{\text{ideal}}} \cdot 100 . \tag{7}$$

shows off as an asymptotic, ideal torque-angle characteristic.

Table 1
The Maximum and Minimum Deviation data for Torque-Angle Characteristics

Deviation, [%]	2-D Model, Design 5, Iron wedges	2-D Model, Design 5, Aluminum wedges
Minimum value	0.081412	0.065784
Maximum value	13.1	16.8411

For Iron wedges in the ±45° operating range the torque-angle curve is approximately linear. For Aluminum wedges the torque-angle characteristic departs from linearity, as shown also through the deviation, Fig. 5.

There is a major difference between the values from the real torque-angle characteristic and the ideal one. At 40° and 45° the deviation values begin to increase because the torque-angle curve becomes a “falling” characteristic (Table 1). This happens as a consequence of saturation, which has a maximum value of 2.38 T, bigger than 2.3 T, which is the maximum value of the magnetic flux density for the same motor design but with Iron wedges.

3. Experimental Results

The analytical and numerical results were validated against an experimental model, shown in Fig. 6.

Fig. 6 – The experimental model of DC-TM.

The stator is provided with terminals, and the rotor is provided with permanent magnets, principal and auxiliary. The stator stack was potted in EP (epoxy) and placed in a metallic case. Because the air gap must be uniform, the torus is placed and centered inside a metallic case with wedges. This process must ensure specified coaxiality.

The experimental model was subjected to a set of measurements and tests specific for DC torque motors in order to obtain torque-angle characteristic within the working range. The working method and the measurement principle are presented in detail by Andrei *et al*. (2014a; 2014b). A comparison between the results of the modeling process and experimental tests is presented in Fig. 7.

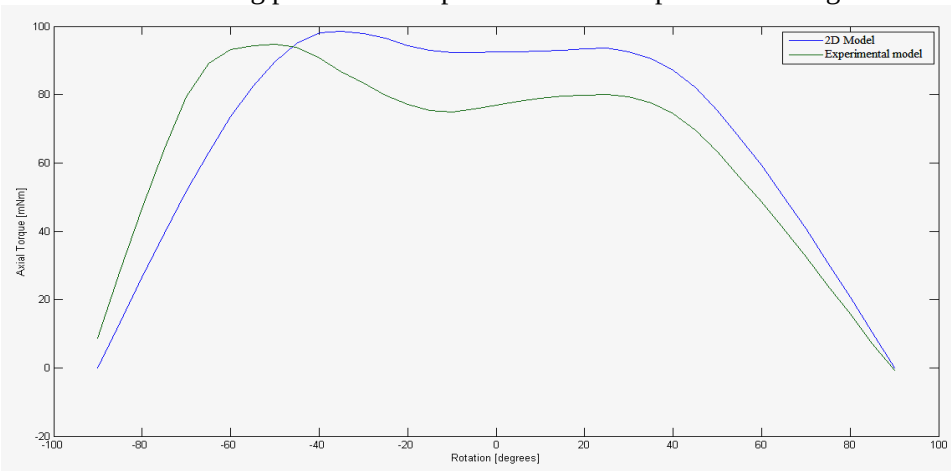

Fig 7 – Torque-angle characteristic comparison.

The tests were performed for the nominal current of 4 A. The numerical models were solved using the same conditions as those of the measurement process. It can be noticed that the torque values of the 2-D model are bigger than the measurements. This happens as a consequence of the simplifying assumptions of the 2-D approximation, including that all components of the model have the same length. The discrepancies between the two characteristics are due also to the material characteristics and the magnetization type.

4. Conclusions

Using the Cobalt-Iron stator stacks made of AFK 502 R sheet limits the saturation level to 2.3 T, and the magnetic flux density in the air gap reaches 0.79 T.

Several designs were used to investigate the effect of increasing the coverage angle of the auxiliary magnets. Thus, the magnetic flux density increases and saturates the stator as the wedges angle decreases (when Iron is used for wedges).

Aluminum wedges (nonmagnetic material) were utilized also: the magnetic field is confined to the iron while the air region is completely avoided.

The torque-angle characteristics for both models were calculated. For Iron wedges, as the wedges angle decreases in a specific angular domain (working field) the torque-angle characteristic is approximately linear. When Aluminum wedges are used, the torque-angle departs from linearity for decreasing wedges angle. The second characteristic should be avoided. It provides for larger values for torque but with poor uniformity.

The deviation of the torque angle characteristic on the operating range of the motor was calculated. For Iron wedges, in the ±45° operating range, the torque-angle characteristic is approximately linear. For Aluminum wedges, the torque-angle characteristic departs from linearity, a conclusion that results also from the deviation, whose data is far as values.

There is a major difference between the real torque-angle characteristic and the ideal one. At 40° and 45° the deviation values starts to increase because the torque-angle characteristic becomes a “falling” characteristic. This happens as a consequence of saturation, which has a maximum value of 2.38 T, bigger than 2.3 T, the maximum value of magnetic flux density for the same motor design, but with Iron wedges.

Acknowledgments. The first author acknowledges the support provided through the Sectoral Operational Programme Human Resources Development 2007-2013 of the Ministry of European Funds through the Financial Agreement POSDRU/187/1.5/S/155536.

Part of research from this article was presented at the International Conference on Electromechanical and Power Systems, SIELMEN 2015, a joint event organized by the Faculty of Power Engineering - Technical University of Moldova, Faculty of Electrical Engineering - "Gheorghe Asachi" Technical University of Iasi and Faculty of Electrical Engineering - University of Craiova.

REFERENCES

Andrei M.-I., Modreanu M., Guțu M., *Stand de măsură pentru motoare de cuplu cu unghi limitat D-4078*. Procedură de lucru - document intern, 2014b.

Andrei M.I., Modreanu N.M., Guțu M., Ghițulescu L., *Sistem de masură asistat de calculator pentru caracterizarea motoarelor de cuplu cu unghi limitat*. EEA - Electrotehnica, Electronica, Automatica, Edit. ELECTRA, **62**, *3*, Jun-Sep. 2014a, 11-17.

Andrei M.I., Modreanu N.M., *Modelarea numerică a unui motor de cuplu cu unghi limitat cu două canale*. EEA - Electrotehnica, Electronica, Automatica, Edit. ELECTRA, **62**, *1*, 2014, 26-31.

Hemeida A., Sergeant P., *Analytical Modeling of Surface PMSM Using a Combined Solution of Maxwell`s Equations and Magnetic Equivalent Circuit*. IEEE Transactions on Magnetics, **50**, *12*, art. 7027913 (2014).

Jin J.-M., *The Finite Element Method in Electromagnetics*. John Wiley and Sons Publisher, New York, 2002.

Măgureanu R., *Maşini electrice speciale pentru sisteme automate*. Edit. Tehnică, Bucureşti, 1981.

Obreja R., Edu I.R., *Limited Angle Torque Motors Having High Torque Density, Used in Accurate Drive Systems*. Acta Polytechnica, **51**, *5*, 75-83 (2011).

Upadhyay P.R., Rajagopal K.R., *FE Analysis and CAD Of Radial-Flux Surface Mounted Permanent Magnet Brushless DC Motors.* Digests of the IEEE Internat. Magnetics Conf. INTERMAG Asia 2005, April 4-8, 2005, 729-730.

Upadhyay P.R., Rajagopal K.R., *FE Analysis and Computer-Aided Design of a Sandwiched Axial-Flux Permanent Magnet Brushless DC Motor*. IEEE Transactions on Magnetics, **42**, *10*, 3401,3403 (2006).

Upadhyay P.R., Rajagopal K.R., Singh B.P., *Computer Aided Design of an Axial-Field Permanent Magnet Brushless DC Motor for an Electric Vehicle*. J. of Appl. Physics, **93**, *10*, 8689,8691 (2003).

* * * *Componente electromecanice pentru sisteme high tech direct drive realizate cu linii tehnologice flexibile – HTDD.* Raport tehnic, etapa 1.

* * * *Componente electromecanice pentru sisteme high tech direct drive realizate cu linii tehnologice flexibile* – HTDD. Raport tehnic, etapa 2.

* * * Comsol Multiphysics documentation: http://www.comsol.com/.

MODELE DE CÂMP MAGNETIC PENTRU UN MOTOR DE CUPLU DE CURENT CONTINUU

(Rezumat)

Lucrarea îşi propune să prezinte şi să analizeze modele de câmp magnetic pentru motoarele de cuplu de curent continuu, talie 16, prin folosirea unui pachet de programe pentru modelare electromagnetică ce are la bază metoda elementului finit. Astfel, se pot evalua cu precizie ridicată diferite configuraţii pentru o maşină electrică, însă fără a se mai realiza modelul experimental.